Homogeneously precessing domain in ^{3}He-B: formation and properties

2009 J. Phys.: Condens. Matter 21 164202

(http://iopscience.iop.org/0953-8984/21/16/164202)

J. Phys.: Condens. Matter **21** (2009) 164202 (9pp) doi:10.1088/0953-8984/21/16/164202

Homogeneously precessing domain in ^{3}He-B: formation and properties

V V Dmitriev and I A Fomin

P L Kapitza Institute for Physical Problems, 2 Kosygina Street, 119334 Moscow, Russia

E-mail: fomin@kapitza.ras.ru

Received 22 January 2009
Published 31 March 2009
Online at stacks.iop.org/JPhysCM/21/164202

Abstract

The long-range order realized in the superfluid phases of ^{3}He leads to a nonlocal motion of spin in these phases. In the B phase the nonlocality manifests itself in the formation of a homogeneously precessing domain (HPD). This domain is formed under conditions of nuclear magnetic resonance. Within the domain spin precesses coherently—with the same frequency and phase even though the steady magnetic field can be nonuniform. Coherence of precession is maintained by the spin current carried by the condensate of Cooper pairs. The key experiments, revealing the main properties of the HPD and the underlying theory are briefly reviewed in this paper.

1. Introduction

A distinctive property of liquid helium as a physical object is its quantum character. This liquid demonstrates quantum phenomena on a macroscopic scale. The most basic of these phenomena is superfluidity. In a contrast to the classical flow, which emerges as a result of averaging of a random motion of particles, superflow is an ordered—coherent motion of particles, no entropy is carried by this current. Liquid ^{4}He undergoes a superfluid transition at a temperature $T_\lambda \approx 2.17\ K$. The change of symmetry at this transition is characterized by the order parameter, which is a scalar complex function $\psi = |\psi|e^{i\varphi}$. The gauge symmetry is broken at this transition and the long-range order on the phase φ is established. Spatially nonuniform perturbations, which tend to destroy this order, produce a superfluid current (supercurrent) of mass: $j_s \sim \nabla\varphi$, restoring the long-range order.

Properties of another quantum fluid–liquid ^{3}He differ strongly from those of ^{4}He. The difference stems from their statistics. Nuclei of ^{3}He have spin 1/2, and ^{3}He forms a Fermi liquid; it can became superfluid only via Cooper pairing as it is in superconductors. Since the discovery of the superfluidity of ^{3}He [1] we know that it happens in the millikelvin temperature range. The Cooper pairs in ^{3}He are qualitatively different from 'conventional' superconductors. Two fermions with spin 1/2 can form the Cooper pair either in a singlet state—with a total spin 0, or in a triplet state—with spin 1. The former case is realized in conventional superconductors, the latter in the superfluid ^{3}He. Formal description of a state with the triplet type of Cooper pairing requires three complex amplitudes—one for each z-projection of spin 1, 0, −1:

$$\Psi = \begin{pmatrix} \psi_{\uparrow\uparrow} \\ \frac{1}{\sqrt{2}}(\psi_{\uparrow\downarrow} + \psi_{\downarrow\uparrow}) \\ \psi_{\downarrow\downarrow} \end{pmatrix}. \tag{1}$$

The arrows here indicate the orientations of the spins of individual quasi-particles, bound in the Cooper pair. This form of the order parameter suggests the possibility of spin transport by the condensate of Cooper pairs, independent of the mass transport. As an illustrative example consider the order parameter, for which zero spin projection on an axis of quantization is absent and two other projections have equal amplitudes [2]:

$$\Psi = |\Psi|e^{i\varphi} \begin{pmatrix} e^{i\gamma} \\ 0 \\ e^{-i\gamma} \end{pmatrix}. \tag{2}$$

In particular, such a form has the order parameter of the A phase of superfluid ^{3}He for the properly chosen direction of the spin quantization axis. Given the order parameter (2) one can separately find currents of up and down components of spin: $j_{\uparrow\uparrow} = (\hbar/2m)|\Psi|^2(\nabla\varphi + \nabla\gamma)$ and $j_{\downarrow\downarrow} = (\hbar/2m)|\Psi|^2(\nabla\varphi - \nabla\gamma)$. Their sum gives the current of mass $j_s \sim \hbar\nabla\varphi$ and the difference—the current of z-projection of spin $j^z_{sp} \sim (\hbar^2/2m)\nabla\gamma$. These currents are independent. The order parameter equation (2) can also be viewed as a ψ-function of a particle with spin 1 and spin projection 0 on a direction

d which is perpendicular to the z-axis. The orientation of **d** in the plane perpendicular to z is determined by the phase γ. When γ varies vector **d** rotates about the z-direction. For a state with a constant spin current the end of **d** traces out a helix with a pitch $2\pi/|\nabla\gamma|$ and the axis oriented along $\nabla\gamma$. Speaking formally, spontaneous breaking of gauge symmetry (phase φ) at the superfluid transition makes possible a flow of mass supercurrent, while spontaneous breaking of the spin rotation symmetry (angle γ) that of spin supercurrent.

The considered situation, when only one direction **d** describes the local spin structure of the order parameter is exceptional. In a general case components of the triplet order parameter equation (1) are complex functions of the wavevectors $\hat{\mathbf{k}}$ of the Fermi-particles, bound into the Cooper pair. A structure of condensate of Cooper pairs is specified by a set of vectors $\mathbf{d}(\hat{\mathbf{k}})$. In ^{3}He Cooper pairs are formed in a state with the orbital angular moment 1, meaning that each of the three spin components of the order parameter is a linear combination of projections $\hat{k}_x, \hat{k}_y, \hat{k}_z$.

If spin–orbit interaction is neglected rotation of a spin vector **d** with respect to its 'orbital' argument $\hat{\mathbf{k}}$ does not change the energy of the state. This rotation can be parameterized by the Euler angles, determined as: $\mathbf{R}(\alpha,\beta,\gamma) = R_z(\alpha)R_y(\beta)R_z(\gamma)$, where $R_z(\gamma)$ is the matrix of rotation at the direction $\hat{z}$ for an angle γ etc. In other words at a triplet Cooper pairing the condensate of Cooper pairs, in addition to the degeneracy with respect to the phase φ, is degenerate with respect to three more parameters: α, β, γ, their variation in space creates spin current, which tends to restore a uniform state. The following combinations of gradients of α, β, γ have the meaning of spin superfluid velocities:

$$\begin{aligned} v^{\rm sp}_{1j} &= \frac{\hbar}{2m_3}(-\sin\alpha\nabla_j\beta + \cos\alpha\sin\beta\nabla_{j\gamma}),\\ v^{\rm sp}_{2j} &= \frac{\hbar}{2m_3}(\cos\alpha\nabla_j\beta + \sin\beta\cos\alpha\nabla_{j\gamma}),\\ v^{\rm sp}_{3j} &= \frac{\hbar}{2m_3}(\nabla_j\alpha + \cos\beta\nabla_{j\gamma}). \end{aligned} \tag{3}$$

Each of the combinations transports respectively the x, y or z projection of spin. These projections will be denoted here by Greek indices μ, ν etc. The additional kinetic energy is a quadratic combination of the velocities:

$$F_\nabla = \tfrac{1}{2}\rho_{\mu\nu jl}v^{\rm sp}_{\mu j}v^{\rm sp}_{\nu l}. \tag{4}$$

The explicit form of the tensor of spin superfluid densities $\rho_{\mu\nu jl}$ depends on a particular form of the order parameter. The spin current is then determined as

$$j^{\rm sp}_\mu = \frac{\partial F_\nabla}{\partial v^{\rm sp}_{\mu l}}. \tag{5}$$

2. Dipole energy

At that point it has to be mentioned that the parallels between the spin and mass supercurrents can not be extended too far. The essential difference between these two types of transport is that spin, unlike mass, is not an exactly conserved quantity. Spin–orbit interaction can change the total spin of the system. In the case of superfluid ^{3}He spin–orbit coupling originates from the interaction of the dipole magnetic moments of the nuclei of ^{3}He, bound in a Cooper pair. This interaction brings about a macroscopic 'dipole' energy with a potential $U_{\rm D}$, depending on the orientation of spin vector $\mathbf{d}(\hat{\mathbf{k}})$ with respect to $\hat{\mathbf{k}}$, or between the spin and orbital degrees of freedom of the order parameter [2]:

$$U_{\rm D} \sim \int (do_k/4\pi)3|\hat{\mathbf{k}}\cdot\mathbf{d}(\hat{\mathbf{k}})|^2. \tag{6}$$

The continuity equation for spin, even at $\mathbf{H} = 0$, contains on the right-hand side a torque N_λ which is a source or a sink of spin:

$$\frac{\partial S_\mu}{\partial t} + \frac{\partial j^{\rm sp}_{\mu n}}{\partial x_n} = N_\mu. \tag{7}$$

The torque is determined as $N_\mu = -\partial U_{\rm D}/\partial\theta_\mu$, where θ_μ is an infinitesimal rotation conjugated to the spin projection S_μ. The dynamics of spin can be dominated by spin flow if the r.h.s. of equation (7) is negligible. A typical situation is just the opposite. In particular, in the A phase the dipole energy has the following form:

$$U^{\rm A}_{\rm D} = -\frac{\chi\Omega^2_{\rm A}}{2g^2}(\mathbf{d}\cdot\mathbf{l})^2, \tag{8}$$

where χ is the magnetic susceptibility of this phase, g is the gyromagnetic ratio of the ^{3}He nuclei and $\Omega_{\rm A}$ is an experimentally measurable longitudinal resonance frequency, dependent on pressure and temperature. At temperatures well below the superfluid transition temperature $T_{\rm c}$ the frequency $\Omega_{\rm A} \approx 2\pi \times 10^5$ s^{-1}, which corresponds to the Larmor frequency of ^{3}He in a magnetic field $\simeq$30 Oe. The dipole interaction is about four orders of magnitude less strong than the 'binding energy' of the Cooper pair, but it is a principal interaction lifting the degeneracy of the order parameter with respect to rotation of the spin coordinates. In equilibrium vector **d** is 'locked'—it has to be aligned with the orbital vector **l**, which points in the direction of the orbital momentum of the Cooper pair. The spin current term in equation (8) is comparable with the torque $\mathbf{N}_{\rm D}$ when **d** varies on a length scale on the order of the so-called dipole length $\xi_{\rm D} \sim c/\Omega_{\rm A}$, where c is the spin wave velocity. For ^{3}He $\xi_{\rm D} \sim 10^{-3}$ cm. An even stronger variation of the order parameter is needed to make the dipole torque negligible.

In the B phase the order parameter $\mathbf{d}(\hat{\mathbf{k}}) = |\Psi|e^{i\varphi}\hat{\mathbf{R}}\hat{\mathbf{k}}$, where $\hat{\mathbf{R}}$ is a real orthogonal matrix. Its elements, as well as $|\Psi|$ and φ, do not depend on $\mathbf{k}$. An orthogonal matrix can be considered as a matrix of rotation, which transforms direction $\hat{\mathbf{k}}$ in a direction $\hat{\mathbf{d}}$, corresponding to a given $\hat{\mathbf{k}}$. This rotation is often parameterized by a unit vector **n**, which specifies the direction of the rotation axis and rotation angle θ, i.e. $\hat{\mathbf{R}} = \hat{\mathbf{R}}(\mathbf{n},\theta)$. For such a form of the order parameter the dipole energy $U_{\rm D}$ does not lift its degeneracy completely. In terms of **n** and θ:

$$U^{\rm B}_{\rm D} = \frac{8}{15}\frac{\chi\Omega^2_{\rm B}}{g^2}\left(\frac{1}{4} + \cos\theta\right)^2, \tag{9}$$

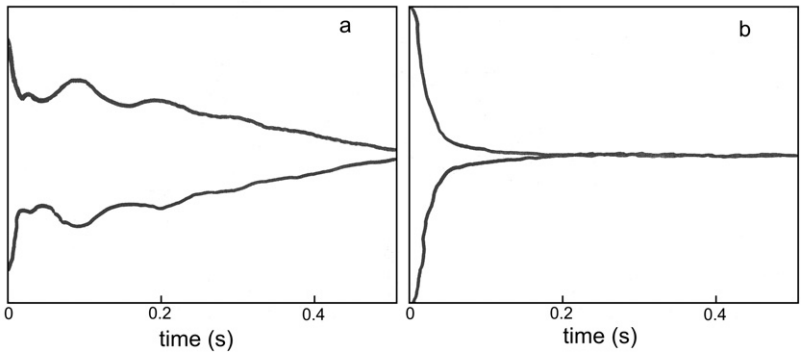

Figure 1. Envelopes of free induction decay signals after a 90° tipping pulse. The cell had the form of a cylinder (⌀5 mm, length of 13 mm) with the axis oriented normal to the external steady field. $P = 29.3$ bar, $H = 77$ Oe. (a) Signal from ^{3}He-B at $T = 0.7$, T_c; (b) signal from normal phase at the same inhomogeneity of **H**.

where Ω_B is the longitudinal resonance frequency in ^{3}He-B. In equilibrium the angle θ takes a value corresponding to the minimum of U_D^B: $\cos\theta = -1/4$, or $\theta = \theta_0 \approx 104°$, but there remains degeneracy with respect to the direction **n**. This degeneracy is ultimately lifted by a much weaker interaction—mutual action of the dipole energy and that of the deformation of the order parameter by the magnetic field **H**, it tends to orient **n** parallel or antiparallel to **H**.

3. Pulsed NMR

Favorable conditions for observation of a macroscopic spin flow are realized in pulsed NMR experiments. In these experiments a steady magnetic field **H** induces equilibrium magnetization $\mathbf{M} = g\mathbf{S} = \chi\mathbf{H}$, where **S** is the spin density of the considered superfluid phase. Thereupon, the magnetization **M** is tilted by an angle β with respect to the equilibrium orientation by the resonant radio frequency (RF) pulse and left to move in the magnetic field. A coupled motion of the spin and of the order parameter $\mathbf{d}(\hat{\mathbf{k}})$ of superfluid ^{3}He is governed by the Leggett equations [3]:

$$\dot{\mathbf{S}} = g\mathbf{S} \times \mathbf{H} + \mathbf{N}_D, \tag{10}$$

$$\dot{\mathbf{d}}(\hat{\mathbf{k}}) = \left(\frac{g^2\mathbf{S}}{\chi} - g\mathbf{H}\right) \times \mathbf{d}(\hat{\mathbf{k}}), \tag{11}$$

which are generated by the Hamiltonian

$$\mathcal{H}_L = \frac{g^2S^2}{2\chi} - g\mathbf{SH} + U_D. \tag{12}$$

Of main interest are effects, originating from the dipole torque $\mathbf{N}_D$. Corruccini and Osheroff [4] were the first to apply the pulsed NMR technique to the superfluid ^{3}He and obtained many interesting results in both superfluid phases. The most important for the present discussion are the results concerning spin precession and magnetic relaxation in ^{3}He-B.

The steady magnetic field in the experiments [4] varied in the range ∼600–1000 Oe. The ratio of the two terms on the r.h.s. of equation (10) scales as $(\omega_L/\Omega_B)^2 \sim 30$–100. The dipole torque produces a small shift of the precession frequency ω_p from the Larmor frequency ω_L. The observed dependence of the shift on the tipping angle β was close to that found theoretically by Brinkman and Smith [5]. For $\beta < \theta_0$ there was no shift, for $\beta > \theta_0$ the shift was positive and it was satisfactorily described by the formula:

$$\omega_p = \omega_L - \frac{4\Omega_B^2}{15\omega_L}(1 + 4\cos\beta). \tag{13}$$

At temperatures below $0.6T_c$ Corruccini and Osheroff observed a very long lived induction signal. The signal appeared after tipping the magnetization through an angle ∼90°, it was about 1/10 of the initial signal in the amplitude, and it persisted for about 1 s. This time is much longer then the dephasing time due to the inhomogeneity of the magnetic field **H**, which was ∼15 ms in these experiments. Later the long lived induction decay signal (LLIDS) was also observed by Giannetta *et al* at different pressures and at higher temperatures $\geqslant 0.75T_c$ [6]. In their experiments the ringing continued for about 50 ms versus the dephasing time (as measured in the normal phase) of about 3.5 ms.

In 1984 a systematic studies of this phenomenon were done in the Kapitza Institute in Moscow. The new element was a possibility to apply a controlled gradient of magnetic field. It is also important that the experimental cells used in the Moscow experiments were almost 'closed', i.e. the experimental volume where spin precession occurred was connected with the rest of the experimental chamber by a long and narrow channel [7, 8]. In figure 1 envelopes of free induction decay signals (FIDS) obtained in such an almost closed cell are shown. As in [4, 6], it was found that for large tipping pulses duration of the FIDS in ^{3}He-B is much longer than in the normal phase at the same inhomogeneity of **H**. For large field gradients the LLIDS persisted up to three orders of magnitude longer than the dephasing time. At the same time the amplitude of the LLIDS was much larger than in the previous experiments (up to 95% of the initial amplitude of the FIDS). It was also observed that the frequency of the LLIDS decreases with time. The rate of the decrease grew with the field gradient. The obtained results clearly indicated that the local precession picture has only limited applicability to describing the motion of magnetization in ^{3}He-B. Nevertheless a closer look at uniform precession is useful as a starting point for constructing a more realistic picture.

4. Coherent precession of spin

The regular precession of $\mathbf{S}$ and $\mathbf{d}(\hat{\mathbf{k}})$ is analogous to precession of a top. This motion is conveniently described in terms of the Euler angles. The instantaneous orientation of the order parameter $\mathbf{d}(\hat{\mathbf{k}}, t)$ is related to its initial orientation $\mathbf{d}_0(\hat{\mathbf{k}})$:

$$\mathbf{d}(\hat{\mathbf{k}}, t) = \hat{\mathbf{R}}(\alpha, \beta, \gamma)\mathbf{d}_0(\hat{\mathbf{k}}). \tag{14}$$

As a $\mathbf{d}_0(\hat{\mathbf{k}})$ the equilibrium orientation of the order parameter can be chosen. The angles α, β, γ are functions of time t. For the sake of definiteness $\mathbf{n}$ is assumed to be antiparallel to the magnetic field. Hamiltonian (12) has to be expressed in terms of α, β, γ and their canonically conjugated projections of spin respectively S_z, S_ζ, S_β, where S_z is the projection on the z-axis, S_ζ the projection on $\hat{\zeta} = \hat{\mathbf{R}}(\alpha, \beta, \gamma)\hat{z}$ and S_β the projection on the direction $\hat{\zeta} \times \hat{z}$. Of the three terms in the Hamiltonian only the dipole energy contains angles α and γ and these angles enter U_D only as a combination $\Phi = \alpha + \gamma$:

$$U_\mathrm{D} = \frac{2}{15}\frac{\chi\Omega_\mathrm{B}^2}{g^2}\left[\cos\beta - \frac{1}{2} + (1+\cos\beta)\cos(\alpha+\gamma)\right]^2. \tag{15}$$

It is convenient to introduce α and Φ as new variables, then their conjugated momenta are $P = S_z - S_\zeta$ and S_ζ respectively. Since the angle α does not enter the Hamiltonian (12) its conjugated momentum $P = S_z - S_\zeta$ is conserved even in a presence of the dipole interaction. In terms of these variables the equations of motion (10), (11) have the standard Hamiltonian form:

$$\begin{aligned} \frac{\partial\alpha}{\partial t} &= \frac{\partial\mathcal{H}_\mathrm{L}}{\partial P} & \frac{\partial P}{\partial t} &= 0 \\ \frac{\partial\beta}{\partial t} &= \frac{\partial\mathcal{H}_\mathrm{L}}{\partial S_\beta} & \frac{\partial S_\beta}{\partial t} &= -\frac{\partial\mathcal{H}_\mathrm{L}}{\partial\beta} \\ \frac{\partial\Phi}{\partial t} &= \frac{\partial\mathcal{H}_\mathrm{L}}{\partial S_\zeta} & \frac{\partial S_\zeta}{\partial t} &= -\frac{\partial\mathcal{H}_\mathrm{L}}{\partial\Phi}. \end{aligned} \tag{16}$$

The advantage of Euler angles as variables is that for a regular precession, in a principal order on a small ratio $(\Omega_\mathrm{B}/\omega_\mathrm{L})^2$, they have a direct physical meaning: β is a 'tipping' angle, i.e. it is the angle between the instantaneous orientation of spin $\mathbf{S}$ and its equilibrium orientation, the angle α is the phase of precession, and the angle γ is the phase of rotation of the order parameter at the instantaneous direction of $\mathbf{S}$. A stationary precession with the frequency ω_p is described by solutions of equations (16) with

$$\frac{\partial\alpha}{\partial t} = -\omega_\mathrm{p}, \qquad \frac{\partial\Phi}{\partial t} = \frac{\partial\beta}{\partial t} = \frac{\partial S_\zeta}{\partial t} = \frac{\partial S_\beta}{\partial t} = 0. \tag{17}$$

According to equations (16) these solutions are minima of the potential

$$\tilde{\mathcal{H}} = \mathcal{H}_\mathrm{L} + P\omega_\mathrm{p} \tag{18}$$

with respect to the variables β, Φ, P etc. Transformation (18) is analogous to the transition from density (P) to chemical potential ($-\omega_\mathrm{p}$) as a variable in thermodynamics, it also makes it possible to consider spatially nonuniform stationary states.

In the general case for a given ω_p potential $\tilde{\mathcal{H}}(S_\zeta, P, S_\beta, \beta, \Phi)$ as a function of its 5 arguments has isolated minima. This is true for the Leggett Hamiltonian of ^{3}He-B only if $\omega_\mathrm{p} > \omega_\mathrm{L}$ [9]. The value $\omega_\mathrm{p} = \omega_\mathrm{L}$ is degenerate—to this value corresponds a whole line of minima. If the tipping angle β is chosen as a parameter on this line the other variables (in units for which $\chi = g^2$) are expressed as: $S_\zeta = \omega_\mathrm{L}$, $S_\beta = 0$, $P = \omega_\mathrm{L}(\cos\beta - 1)$ and the angle Φ has two branches $\pm\Phi(\beta)$, determined by the equation:

$$\cos\Phi = \frac{1/2 - \cos\beta}{1 + \cos\beta}. \tag{19}$$

Meaningful solutions of this equation exist for $0 \leqslant \beta \leqslant \theta_0$. On the line of minima $U_\mathrm{D}^\mathrm{B} = 0$ and $\tilde{\mathcal{H}}(S_\zeta, P, S_\beta, \beta, \Phi) = \mathrm{const}$. Degeneracy of $\tilde{\mathcal{H}}$ at $\omega_\mathrm{L} - \omega_\mathrm{p} = 0$ with respect to $\cos\beta$, or to the variable $P = \omega_\mathrm{L}(\cos\beta - 1)$, which is conjugated to $\omega_\mathrm{L} - \omega_\mathrm{p}$, is analogous to the degeneracy of the state of the ideal Bose-gas at $\mu = 0$ with respect to its density. In case of a Bose-gas this degeneracy results in Bose–Einstein condensation. For the precessing spin the analogous degeneracy gives rise to formation of coherently precessing structures [10, 11].

When β grows from 0 to θ_0 the angle Φ varies from $\pm\theta_0$ to 0. At $\beta = \theta_0$ two branches of $\Phi(\beta)$ merge and in the interval $\theta_0 < \beta < \pi$ $\Phi(\beta) = 0$. In this interval of β the dipole energy grows from 0 at $\beta = \theta_0$ to $3\chi\Omega_\mathrm{B}^2/(10g^2)$ at $\beta = \pi$. In both intervals of β combination $\Phi = \alpha + \gamma$ is fixed, i.e. the phase of rotation of the order parameter γ is rigidly connected with the phase of precession of spin α. The precessing configurations of spin and of the order parameter are uniquely determined by the two angles α and β.

The degeneracy of a state of precession with $\omega_\mathrm{p} = \omega_\mathrm{L}$ is lifted by inhomogeneity of magnetic field. For definiteness here, and in what follows, we consider the simplest form of inhomogeneity—a constant field gradient, i.e. the Larmor frequency is linearly changing along direction z, coinciding with the direction of the magnetic field:

$$\omega_\mathrm{L}(z) = \omega_\mathrm{L}(z_0) + (z - z_0)\nabla\omega_\mathrm{L}, \tag{20}$$

where z_0 is defined by the condition: $\omega_\mathrm{L}(z_0) = \omega_\mathrm{p}$. The analysis can be easily reformulated for more complicated configurations of the field. Neglecting the effect of side boundaries we consider a stationary solution, depending only on one coordinate—z. This solution is an extremum of the functional

$$\int [\tilde{\mathcal{H}}|_{\omega_\mathrm{L}(z_0)} - (z - z_0)S_z\nabla\omega_\mathrm{L} + F_{B\nabla}]\,\mathrm{d}z. \tag{21}$$

Here $F_{B\nabla}$ is the kinetic, or 'gradient' energy (4) specified for the B phase. In the one-dimensional case it has the form:

$$\begin{aligned} F_{B\nabla} = {} & \tfrac{1}{2}c_\parallel^2[2(1-\cos\beta)\alpha'(\alpha' - \Phi') + \Phi'^2 + \beta'^2] \\ & - (c_\parallel^2 - c_\perp^2)[(1-\cos\beta)\alpha' - \Phi']^2, \end{aligned} \tag{22}$$

where $c_\parallel$ and $c_\perp$ are the velocities of the two types of spin-waves in ^{3}He-B. To simplify the formula here we use units such that $g^2 = \chi$. Inhomogeneity of the field is usually small ($\sim$1 Oe cm^{-1}) making it possible to treat in (21) the terms containing $\nabla\omega_\mathrm{L}$ and derivatives of the angles α', β' and Φ' as perturbations. As the zero-order approximation the degenerate

minimum of $\tilde{\mathcal{H}}|_{\omega_L=\omega_p}$ has to be used: $S_z = \omega_p \cos\beta$, $S_\zeta = \omega_p$, $S_\beta = 0$ and $\Phi(\beta)$, given by equation (19). For this solution $\tilde{\mathcal{H}}|_{\omega_L=\omega_p} = \text{const}$. and only the part of the functional (21) containing perturbation has to be minimized with respect to the angles α and β over which the zeroth-order solution is degenerate:

$$\delta \int [F_{B\nabla} - \omega_p \cos\beta(\nabla\omega_L)(z - z_0)]\,dz = 0. \qquad (23)$$

The general form of the solution can be guessed even without solving the corresponding variational problem. The second term in the integrand has the minimum possible value if $\cos\beta = 1$ for $z > z_0$ and $\cos\beta = -1/4$ for $z < z_0$. The gradient energy $F_{B\nabla}$ leads to a smooth transition between the two limiting values of β. One can conclude, that in a weakly inhomogeneous magnetic field stationary precession with the frequency ω_p is realized in the form of the spatially nonuniform spin structure [12, 13]. The structure consists of two domains, separated by the domain wall situated at $z = z_0$, defined by the condition $\omega_L(z_0) = \omega_p$. In a region of z, corresponding to stronger magnetic field spin has equilibrium orientation (equilibrium domain), while in a region of weaker field the spin is tilted by an angle $\beta \approx \arccos(-1/4)$ and precesses with the angular velocity ω_p (figure 2).

To maintain a constant ω_p when ω_L varies with coordinates in the precessing domain spin has to be tilted by an angle $\beta > \theta_0$. In this region $\Phi(\beta) = 0$ and the emerging dipole shift compensates variation of ω_L. According to equation (13) the angle β tends to

$$\beta = \theta_0 + \left(\frac{15}{16}\right)^{1/2} \frac{\omega_L \nabla\omega_L}{\Omega_B^2}(z_0 - z), \qquad (24)$$

when $z_0 - z$ decreases. For typical experimental conditions the maximum deviation of tipping angle from θ_0 within the precessing domain is small $(\beta_{max} - \theta_0) \leqslant 0.1$ rad.

A more detailed analysis of the two-domain structure can be carried out with the use of Euler–Lagrange equations, corresponding to the functional (23). Variation of the functional (23) with respect to α gives the equation

$$\frac{\partial}{\partial z}\{(\cos\beta - 1)[2\alpha'(c_\parallel^2 \cos\beta + (1 - \cos\beta)c_\perp^2) + \Phi'(2c_\perp^2 - c_\parallel^2)]\} = 0. \qquad (25)$$

This is a conservation law (7) for $P = S_z - S_\zeta$ in the case of stationary flow. The combination of derivatives in the curly brackets is the expression for the current of P in the direction z: j_{Pz}^{sp}. According to equation (25) $j_{Pz}^{sp} = \text{const}$. The constant here is determined by the boundary conditions. It is natural to assume, that at the boundaries of the container, oriented perpendicular to the z-direction $j_{Pz}^{sp} = 0$, then for a closed container $j_{Pz}^{sp} = 0$ everywhere inside the container. Taking into account that within the precessing domain $\Phi = 0$ we arrive at the conclusion, that in this domain $\alpha = \text{const}$.. That means that not only frequency, but also the phase of precession is constant even though the magnetic field in not uniform. This property is sometime referred to as the *coherence* of precession. To emphasize this property the abbreviation HPD (homogeneously precessing domain) is used. It is clear from the above discussion that for the HPD formation the geometry of the cell is important. If the cell is not 'closed' then the condition $j_{Pz}^{sp} = 0$ may not be fulfilled and the HPD may not be formed or can be formed only for a specific inhomogeneity of the steady magnetic field.

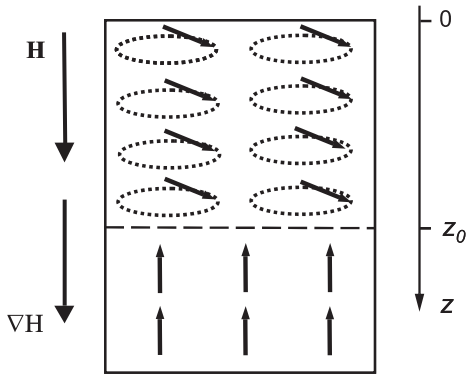

Figure 2. Schematic drawing of the two-domain structure. The arrows on the figures point in the direction of the spin density **S**. It should be remembered that g is negative and the magnetization $\mathbf{M} = g\mathbf{S}$ is counter-aligned with **S**.

Within the HPD the phase of precession α is analogous to the phase of the order parameter $\psi = |\psi|\exp(i\varphi)$ for the superfluid ^{4}He. The spin current maintains coherence of precession analogous to the mass current, which in the case of ^{4}He maintains a constant φ. Perturbations of the phase α give rise to oscillations of the structure involving spin and spin current. The experimentally measured frequency of these oscillations agrees with the theoretical calculations [14, 15].

Variation of the functional (23) with respect to β gives the second Euler–Lagrange equation which makes it possible to find the variation of angles α and β within the domain wall. Numerical solution of the obtained equation, together with equation (25), gives a smooth curve for a change of $\cos\beta$ from 1 to $(-1/4)$ within a region with a characteristic length $\lambda = [c_\parallel^2/(\omega_p \nabla\omega_L)]^{1/3}$ (cf curves 4, 5, 6 in figure 4). For $H_0 \approx 300$ Oe, $\nabla H_0 \approx 0.1$ Oe cm^{-1}, $c_\parallel \approx 1000$ cm s^{-1}, $\lambda \approx 4 \times 10^{-2}$ cm.

5. Formation and relaxation of the HPD

The described two-domain structure is stationary only while dissipative processes are neglected. For a small dissipation it becomes quasi-stationary. Within the structure only the precessing domain is out of equilibrium. The approach to the equilibrium has to go via an increase of the equilibrium domain at the expense of the precessing domain. In this process the domain wall has to move in the direction of the weaker magnetic field, and because of the condition $\omega_p = \omega_L(z_0)$ the frequency of precession of the two-domain structure decreases with time, in agreement with the observation [7, 8]. The major contribution to the relaxation of the structure comes from the two mechanisms of relaxation of spin: spin diffusion across the domain wall and the Leggett and Takagi 'intrinsic' mechanism of relaxation, which is effective within the precessing domain.

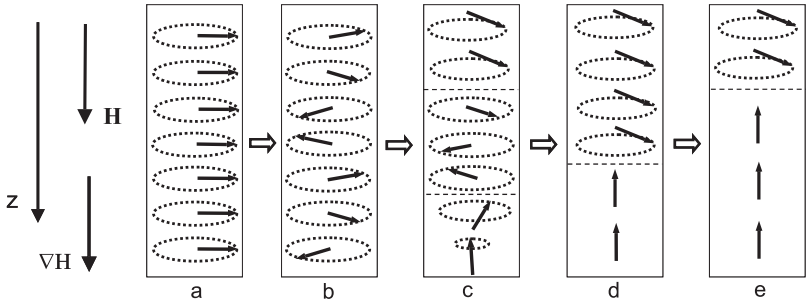

Figure 3. Formation and relaxation of the HPD after the 90° tipping pulse. At the beginning the dephasing (b) results in flow of spin along the z-axis $j^{sp} \propto \nabla\alpha$ and in redistribution of spin (c): near the top β reaches ∼104°, while near the bottom $\beta = 0$. Then the domain wall is formed (d), so that $j^{sp} = 0$. The magnetic dissipation results in a gradual decrease of the HPD size ((d)–(e)).

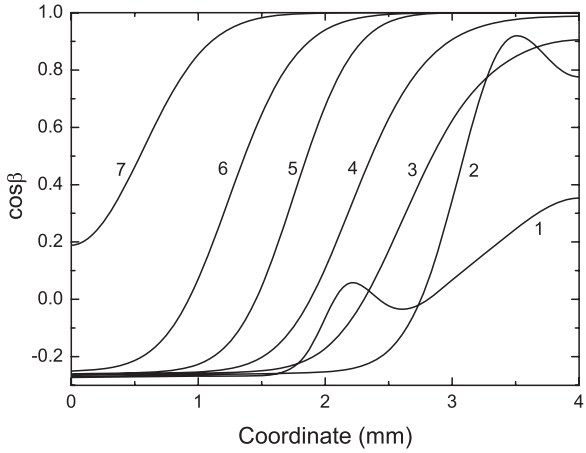

Figure 4. Computer simulations of the HPD formation and relaxation in the pulsed NMR experiment. The curves show the spatial distribution of $S_z = \cos\beta$ in a 4 mm long cell at different times after the 90° tipping pulse: 1–4 ms, 2–8 ms, 3–14 ms, 4–30 ms, 5–46 ms, 6–62 ms, 7–94 ms. The duration of the corresponding LLIDS is about 100 ms. The parameters of the simulations are: $H = 284$ Oe, $\nabla H = 0.2$ Oe cm^{-1}, $P = 16$ bar, $T = 0.54T_c$, $D = 0.02$ cm^2 s^{-1}.

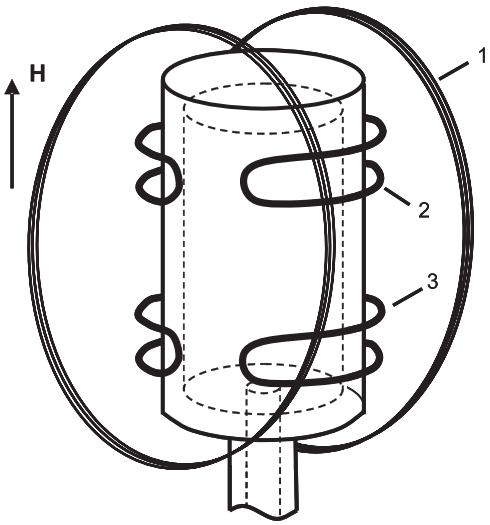

Figure 5. Sketch of the cell with three NMR coils.

The sum of both contributions in the hydrodynamic limit gives the following rate of a change of precession frequency:

$$\frac{d\omega_p}{dt} = -\frac{4}{5}\frac{D_1}{\lambda}\sigma\nabla\omega_L - \frac{1}{4}\tau_{eff}[\omega_p - \omega_L(0)]^3, \qquad (26)$$

where D_1 is a relevant component of the spin diffusion tensor and τ_{eff}—a phenomenological constant, which characterizes the efficiency of the Leggett and Takagi mechanism of relaxation. The contribution of this mechanism to the rate of relaxation depends strongly on the total variation of the Larmor frequency over the length of the precessing domain $\omega_p - \omega_L(0)$ (it is assumed here that $z = 0$ corresponds to the low-frequency end of the cell). The contribution of spin diffusion in equation (26) does not depend on the position of the domain wall, making it possible to separate the two contributions and extract from the experimental data the dissipative constants τ_{eff} and D_1 [16].

An account of dissipation is also necessary for a description of the process of formation of the two-domain structure from the uniform state of precession, prepared by the usual pulsed NMR technique. A qualitative scenario can easily be guessed (cf figure 3). After the tipping pulse the spin starts to precess with a local Larmor frequency. This frequency is spatially nonuniform, giving rise to a dephasing which increases with time: $\nabla\alpha \approx t\nabla\omega_L$. The dephasing in its turn gives rise to the spin current, which redistributes the spin over the volume of the cell, increasing the z-projection of spin in the part of the container situated in a stronger magnetic field and decreasing it in the opposite part. After damping of the transient oscillations the two-domain structure is formed, which relaxes slowly to complete equilibrium. This scenario is confirmed by a one-dimensional computer simulation of the process of the formation of the structure with the use of a full system of equations of spin dynamics including the spin supercurrent (figure 4).

For experimental verification of the proposed scenario a special cell with three NMR coils was made [7, 8] (figure 5). Coil 1 was used to tip the spin in the whole volume of the cell. The miniature coils 2 and 3 were used to detect the signals separately from the upper and lower parts of the cell (their sensitivity regions did not overlap). Time dependencies of the FIDS amplitude in ^{3}He-B recorded from coils 2 and 3

are shown in figure 6. The clear difference in the signals can be explained as follows. After the large tipping pulse applied to coil 1 it takes about 20 ms for the two-domain structure to be formed. The field gradient is directed so that the precessing domain is formed in the upper part of the cell, i.e. near coil 2. As a consequence the amplitude of the signal from this coil is large. Correspondingly the equilibrium domain, which does not precess, is formed near the coil 3 and the signal from the coil 3 rapidly disappears (figure 6(b)). Magnetic relaxation leads to a gradual decrease of the HPD size: the domain wall is moving up and the signal from coil 2 starts to decrease when the wall enters its region of sensitivity (figure 6(a)). It should also be noted that variation of the frequency of the signal with time corresponds well to the HPD model: after formation of the two-domain state the frequency decreases and the total change of the frequency is equal to $l\nabla\omega_{\mathrm{L}}$, where l is the initial length of the HPD, which does not exceed the cell length and depends on the initial tipping angle. When the direction of $\nabla\omega_{\mathrm{L}}$ was reversed the signals in the coils 2 and 3 exchanged their roles, except that the LLIDS in the coil 3 did not last as long as in the coil 2. The difference can be attributed to the leakage of the precessing spin through the connecting tube at the bottom of the cell.

The pulsed NMR experiment with three coils was the first direct experimental verification of the existence of the two-domain structure. It also confirmed the main properties of the structure. Further possibilities for investigation and application of the two-domain structure were opened by the use of the continuous wave (CW) NMR technique. It was found that a sufficiently strong resonant radio frequency field can compensate the energy dissipated in the two-domain structure. With this technique the HPD can be maintained as long as necessary. The power absorbed by precessing magnetization from the RF field is defined by the following equation:

$$W = \tfrac{1}{2}\int h\omega_{\mathrm{RF}}|\mathbf{M}|\cos\beta\sin(\alpha-\phi)\,\mathrm{d}V, \qquad (27)$$

where h is the amplitude of the RF field and ϕ is the phase of RF field. For large enough h the phase of precession α can tune itself to the phase of RF field so that the power W becomes equal to that dissipated in the HPD. The condition $\omega_{\mathrm{p}} = \omega_{\mathrm{RF}} = \omega_{\mathrm{L}}(z_0)$ defines the 'effective' position of the domain wall in figure 2 as $z_0 = (\omega_{\mathrm{RF}} - \omega(0))/(\nabla\omega_{\mathrm{L}})$, which can be inside or outside of the cell. Inside the cell the effective position coincides with the position of the real domain wall. By varying ω_{RF} one can create the two-domain structure and change the position of the domain wall [17]. In practice, it is more convenient to vary ω_{L} (i.e. H) than ω_{RF}. For the creation of the HPD it is important whether H_0 is increased or decreased. If for the geometry shown in figure 2 the effective position z_0 moves downwards (i.e. H_0 is decreasing) and enters the cell at the top then the HPD is created and grows. But if z_0 moves upwards (in the absence of the HPD) and enters the cell at the bottom the HPD is not created, because now it should be created at once in the whole volume of the cell. Thus the CW NMR signal from the HPD is characterized by hysteresis with respect to the direction of the sweep. We should remark here that the hysteretic behavior in nonlinear CW NMR in ^{3}He-B

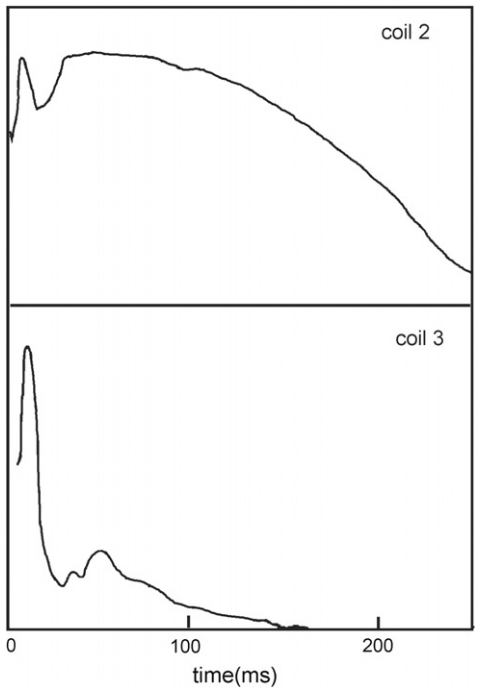

Figure 6. Amplitudes of free induction decay signals from the HPD recorded from coil 2 and coil 3 after the tipping pulse applied by coil 1. The magnetic field gradient was applied so that the HPD should be formed in the upper part of the cell. $P = 29.3$ bar, $H = 142$ Oe, $\nabla H = 0.1$ Oe cm^{-1}, $T = 0.63$, T_{c}.

was previously observed in [18, 19], but it is not clear whether it was due to the HPD or to a complex spatial distribution (texture) of the order parameter. In experiments [17] the existence of the HPD formation in CW NMR was verified by the following procedure: after the HPD formation, the CW RF field was switched off and the LLIDS, corresponding to a slow relaxation of the HPD, was observed.

6. Applications of HPD

In further experiments the two-domain structure was used as a tool for investigations of other phenomena which involve spin currents. In the experiments with one HPD some of the parameters, characterizing properties of the superfluid ^{3}He, were measured, such as the above mentioned relaxation constants D_{l} and τ_{eff} and the spin wave velocities $c_{\parallel}$ and $c_{\perp}$ [8, 16, 20]. It was also found that the HPD interacts with rotating ^{3}He-B. That allowed the study of the structure of vortices [21, 22] and the measurement of the superfluid density anisotropy [23].

According to equation (27) for a fixed length of HPD (or, equivalently, of the rate of dissipation) an increase of h results in a decrease of $|\alpha - \phi|$. In practice, for standard parameters $\alpha \approx \phi$ already at $h \geqslant 0.01$ Oe. This makes it possible to control α in the HPD by the RF field. This possibility was used for studies of the flow of spin supercurrent through the channel connecting two separate cells with HPDs maintained by independent RF fields [24, 25]. When the phases of precession in these two HPDs were different the

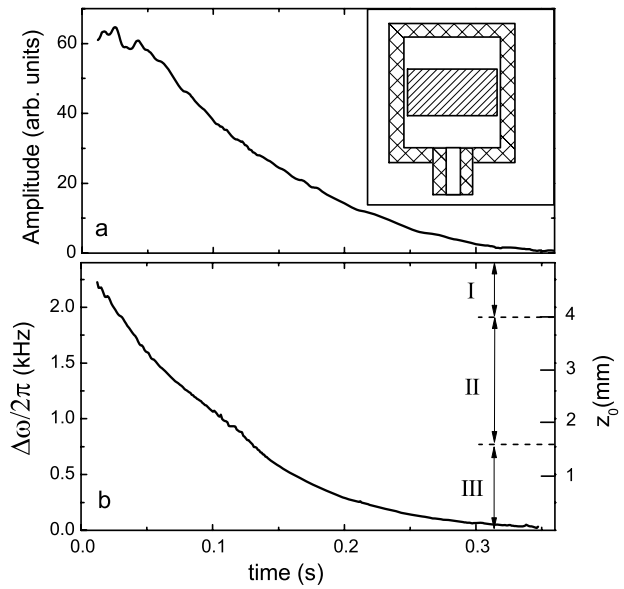

Figure 7. Amplitude (a) and frequency (b) of LLIDS from the HPD in the 'sandwich' cell shown in the inset. The cell had a diameter of 5.3 mm and a length of 5.6 mm. The aerogel disc had a thickness of 2.4 mm and was situated in the middle. The scale at the right axis of the lower graph shows the approximate position of the domain wall calculated from the frequency using equation (20). The initial HPD length is 4.6 mm, $H = 284$ Oe, $\nabla H = 1.6$ Oe cm^{-1}, $P = 25.5$ bar, $T \approx 0.5$, T_{ca}, where T_{ca} is the temperature of the superfluid transition of ^{3}He in aerogel, which was equal to about 0.8 of the temperature of the superfluid transition in the bulk ^{3}He.

spin supercurrent in the channel was excited. The dependence of spin supercurrent on the phase difference was measured. Phase slips and the transition to Josephson phenomena on spin current were observed as well.

The HPD is specific for the B phase order parameter and can be used as its 'signature'. In the B-like phase of ^{3}He in aerogel, whose order parameter is analogous to that of the bulk ^{3}He-B, the HPD has also been observed and used for measurements of Ω_B [26, 27]. The temperature of superfluid transition of ^{3}He in aerogel is essentially smaller than in the bulk ^{3}He; the gap and other parameters (spin wave velocities, Leggett frequency etc) are also different. However, in a special 'sandwich' cell (inset in figure 7), where both the bulk B phase and B-like phase in aerogel were present, it was possible to create one common HPD in the whole volume. The HPD was created by CW NMR and was grown to occupy the whole volume. The amplitude and frequency of LLIDS recorded after switching off the RF field are shown in figure 7. It is seen that the HPD relaxation (i.e. the decrease of its length) occurs without any sharp features: at the beginning the domain wall moves inside the bulk ^{3}He-B (region I in figure 7), then inside aerogel (region II) and, finally, again in the bulk ^{3}He-B (region III). It demonstrates that HPDs in bulk ^{3}He and in ^{3}He in aerogel have the same structure which is defined mainly by the form of the order parameter, but not by its quantitative characteristics.

In conclusion we would like to mention that the HPD is the most simple and best understood example of coherently precessing spin structures maintained by spin supercurrents. At temperatures below $\sim 0.3T_c$ a very long lived induction signal with properties, different from these of the HPD, was observed [28]. It is referred as the 'persistent' signal in the literature. According to the existing interpretation this signal originates from the coherent precession of the spin within a localized region with a size which is much smaller than the size of the experimental cell. This precessing pattern is trapped by the texture of the order parameter [29, 30]. In this case the coherence of precession is also maintained by the spin supercurrent. Further possibilities of realization of coherent precession including A and B phases with a special orientation of their order parameters [31–33] have been discussed. However, to date no experimental evidence of such coherently precessing structures has been reported.

Acknowledgments

We pay great homage to the memory of A S Borovik-Romanov who initiated the experimental investigations of superfluid ^{3}He in the Kapitza Institute and for many years supervised this research. We thank Yu M Mukharskii for his substantial contribution to the majority of the experimental results described in this paper. We also acknowledge a fruitful collaboration with our colleagues from different countries and institutes.

The work on this paper and on some of the recent results was supported by the RFBR grants (07-02-00214 and 06-02-17185) and by the Ministry of Education and Science of Russia.

References

[1] Osheroff D D, Richardson R C and Lee D M 1972 *Phys. Rev. Lett.* **28** 885
Osheroff D D, Richardson R C and Lee D M 1972 *Phys. Rev. Lett.* **29** 920
[2] Leggett A J 1975 *Rev. Mod. Phys.* **47** 331
[3] Leggett A J 1973 *Phys. Rev. Lett.* **31** 352
[4] Corrucini L R and Osheroff D D 1978 *Phys. Rev.* B **17** 126
[5] Brinkman W F and Smith H 1975 *Phys. Lett.* A **53** 43
[6] Giannetta R W, Smith E N and Lee D M 1981 *J. Low Temp. Phys.* **45** 295
[7] Borovik-Romanov A S, Bunkov Yu M, Dmitriev V V and Mukharskii Yu M 1984 *Pis. Zh. Eksp. Teor. Fiz.* **40** 256
Borovik-Romanov A S, Bunkov Yu M, Dmitriev V V and Mukharskii Yu M 1984 *JETP Lett.* **40** 1033 (Engl. Transl.)
[8] Borovik-Romanov A S, Bunkov Yu M, Dmitriev V V, Mukharskii Yu M and Flachbart K 1985 *Zh. Eksp. Teor. Fiz.* **88** 2025
Borovik-Romanov A S, Bunkov Yu M, Dmitriev V V, Mukharskii Yu M and Flachbart K 1985 *Sov. Phys.—JETP* **61** 1199 (Engl. Transl.)
[9] Fomin I A 1983 *Zh. Eksp. Teor. Fiz.* **84** 2109
Fomin I A 1983 *Sov. Phys.—JETP* **57** 1227 (Engl. Transl.)
[10] Fomin I A 1991 *Physica* B **169** 153
[11] Volovik G E 2007 arXiv:cond-mat/0701180
[12] Fomin I A 1984 *Pis. Zh. Eksp. Teor. Fiz.* **40** 260
Fomin I A 1984 *JETP Lett.* **40** 1037 (Engl. Transl.)
[13] Fomin I A 1985 *Zh. Eksp. Teor. Fiz.* **88** 2039
Fomin I A 1985 *Sov. Phys.—JETP* **61** 1207 (Engl. Transl.)
[14] Bunkov Yu M, Dmitriev V V and Mukharskii Yu M 1986 *Pis. Zh. Eksp. Teor. Fiz.* **43** 131

Bunkov Yu M, Dmitriev V V and Mukharskii Yu M 1986 *JETP Lett.* **43** 168 (Engl. Transl.)
[15] Fomin I A 1986 *Pis. Zh. Eksp. Teor. Fiz.* **43** 134
Fomin I A 1986 *JETP Lett.* **43** 171 (Engl. Transl.)
[16] Bunkov Yu M, Dmitriev V V, Markelov A V, Mukharskii Yu M and Einzel D 1990 *Phys. Rev. Lett.* **65** 867
[17] Borovik-Romanov A S, Bunkov Yu M, Dmitriev V V, Mukharskii Yu M, Poddyakova E V and Timofeevskaya O D 1989 *Zh. Eksp. Teor. Fiz.* **96** 956
Borovik-Romanov A S, Bunkov Yu M, Dmitriev V V, Mukharskii Yu M, Poddyakova E V and Timofeevskaya O D 1989 *Sov. Phys.—JETP* **69** 542 (Engl. Transl.)
[18] Osheroff D D 1977 *Proc. Int. Symp. Quantum Fluids and Solids (Sanibel Island, FL)* (New York: Plenum)
[19] Webb R A 1977 *Phys. Rev. Lett.* **39** 1008
[20] Bunkov Yu M, Dmitriev V V and Mukharskii Yu M 1992 *Physica* B **178** 196
[21] Bunkov Yu M and Hakonen P J 1991 *J. Low Temp. Phys.* **83** 323
[22] Kondo Y, Korhonen J S, Krusius M, Dmitriev V V, Mukharsky Yu M, Sonin E B and Volovik G E 1991 *Phys. Rev. Lett.* **67** 81
[23] Bunkov Yu M, Dmitriev V V, Korhonen J S, Kondo Y, Krusius M, Mukharskii Yu M, Parts U and Thuneberg E V 1992 *Phys. Rev.* B **46** 13983
[24] Borovik-Romanov A S, Bunkov Yu M, Dmitriev V V and Mukharskii Yu M 1987 *Pis. Zh. Eksp. Teor. Fiz.* **45** 98
Borovik-Romanov A S, Bunkov Yu M, Dmitriev V V and Mukharskii Yu M 1987 *JETP Lett.* **45** 124 (Engl. Transl.)
[25] Borovik-Romanov A S, Bunkov Yu M, de Waard A, Dmitriev V V, Makrotsieva V, Mukharskii Yu M and Sergatskov D A 1988 *Pis. Zh. Eksp. Teor. Fiz.* **47** 400
Borovik-Romanov A S, Bunkov Yu M, de Waard A, Dmitriev V V, Makrotsieva V, Mukharskii Yu M and Sergatskov D A 1988 *JETP Lett.* **47** 478 (Engl. Transl.)
[26] Dmitriev V V, Zavjalov V V, Zmeev D E, Kosarev I V and Mulders N 2002 *Pis. Zh. Eksp. Teor. Fiz.* **76** 371
Dmitriev V V, Zavjalov V V, Zmeev D E, Kosarev I V and Mulders N 2002 *JETP Lett.* **76** 312 (Engl. Transl.)
[27] Dmitriev V V, Zavjalov V V, Zmeev D E and Mulders N 2004 *Pis. Zh. Eksp. Teor. Fiz.* **79** 612
Dmitriev V V, Zavjalov V V, Zmeev D E and Mulders N 2004 *JETP Lett.* **79** 499 (Engl. Transl.)
[28] Bunkov Yu M, Fisher S N, Guenault A M and Pickett G R 1992 *Phys. Rev. Lett.* **69** 3092
[29] Shaw N S, Cousins D J, Fisher S N, Gregory A I, Pickett G R and Bunkov Yu M 1998 *J. Low Temp. Phys.* **110** 57
[30] Bunkov Yu M and Volovik G E 2007 *Phys. Rev. Lett.* **98** 265302
[31] Bunkov Yu M and Volovik G E 1993 *Europhys. Lett.* **21** 837
[32] Bunkov Yu M and Volovik G E 1993 *Zh. Eksp. Teor. Fiz.* **103** 1619
Bunkov Yu M and Volovik G E 1993 *JETP* **76** 794 (Engl. Transl.)
[33] Fomin I A 1998 *Phys. Lett.* A **249** 330